Ultra-High Spectral Resolution Observations of Fragmentation in Dark Cloud Cores

'J'. **Velusamy[1], W.D. Langer, T.B.H. Kuiper,** S. **Levin, and E.T. Olsen**
Jet Propulsion Laboratory, California Institute of Technology
Mail Stop 169-506, 4800 Oak Grove Drive, Pasadena, CA 91109

Abstract

WC! present new evidence of the fragmentary structure of dense Colts in dark clouds using the high resolution spectra of the carbon chain molecule CCS transition (J_N =- 2_1 - 10) at 22.344033 GIIz made with 0.008 km s^{-1} resolution. The observations utilized NASA's 70-In antenna (spatial resolution of 45 arcsec) and the IIR MS two million channel Wide Band Spectrum Analyzer at Goldstone. The spectra are fully resolved into multiple velocity components, each with intrinsic line-width of 0.15 km s^{-1} or less, slightly larger than the thermal broadening. The spectral line profiles and the position-velocity maps are decomposed into several velocity components (clumps), providing new insight into the clumpiness and velocity structure within the dense cores of cold dark clouds. We interpret these clumps to be stable or quasi-stable fragments approaching the lowest mass (M $\sim$ 0.01 $M_{\odot}$) formed at the culmination of successive fragmentation.

Subject headings: ISM: star formation and fragmentation - ISM: molecules - ISM: dark cloud cores

[1]On leave from Tata Institute of Fundamental Research, Bombay, India

1 Introduction

To understand the dynamics of star forming regions, especially the process of fragmentation in dense molecular cloud cores, it is crucial that we know their velocity and density structure. Despite the fundamental nature of this problem, and although there mists a fair amount of observational data of the cores, relatively little is known shout this process. This lack is mainly due to the observational limitations of spatial and spectral resolution needed to identify individual clumps. In this *Letter* we address one of these limitations using ultra high resolution spectra, sufficient to separate out individual clumps along the line of sight, obtained with NASA'S two million channel Wide Band Spectrum Analyzer (Quirk et al. 1988) and 70-m antenna at Goldstone. We find evidence for many more clumps in individual cores than previously suspected and present new results 011 the fragmentation process in dense cores,

Recently Suzuki et al. (1 992) have shown that the earl.mll chain molecule CCS is widespread in the quiescent dark clouds. The CCS lines arc excellent tracers for investigating the velocity structure in the dense cores, because they have 110 hyperfine structure, are heavy enough to have intrinsically narrow thermal line width (0.1 km s^{-1} at 12 K), require high density for excitation, and arc probably not too opaque. Such intrinsic narrow thermal line widths afford better separation of velocity structure of individual components than lines of CO, ammonia, and most other molecular tracers. Wc utilized these properties of CCS as a tracer of clumpiness in a systematic survey of the cores of cold dark clouds in the $J_N = 2_1 - 1_0$ transition at 22.344033 GHz with velocity resolution of 0.008 km s^{-1}. The multiple velocity components apparent in these spectra can be interpreted as evidence for very low mass fragments which make up the larger structures. Here we present some of the high resolution spectra, analyze the separation of the clumps within the cores, and report direct observational evidence for Presence of low mass clumps formed after successive fragmentation.

2 Observations

The CCS spectral line observations of dark C.1OUC1 cores were made between 13 March and 25 June 1993, using NASA 70 in-a]ltcllla at Goldstone, California. At 22 GHz the aperture efficiency was about 45% at 50° elevation, the antenna HPBW was 45 arcsec and the pointing accuracy was better than 5 arcsec. The overall system noise was about 60 K. We used the High Resolution Microwave Survey (HRMS) two million channel, Wide Band Spectrum Analyzer with a spectral resolution of 19 Hz over 40 MHz. The spectra were taken by observing ON and OFF source positions for 5 to 10 minutes. DR 21 was used for antenna calibrations. The spectral resolution was reduced by adding adjacent 32 channels together to provide 8192 channels of resolution 0.610 kHz (0.008 km s-'), and all 8192 outputs were stored. The spectra were doppler corrected to an accuracy better than O.OO4 km s^{-1}. The LO frequency was maintained by a reference frequency standard hydrogen maser. The spectra averaged over the data taken at different times and 011 different days show smearing of about 0.01 km s^{-1}.

We have observed the spectra in six dark cloud cores (listed in Table 1) which have the brightest emission in the CCS survey of Suzuki et al (1992), and have mapped a few of them. The observed positions arc indicated in Fig.1. These spectra were taken with total

integration times of 45 to 100 minutes for the centers of cores and 20 to 40 minutes for other positions in the mapping grid. For absolute calibration of the intensity scale of the spectra we have used the integrated spectral line temperatures of some of the positions given by Suzuki et al. (1 W?).

3 Results

3.1 Spectral line profile

Figure 1 shows some of the spectra observed in the dark cloud corm, and Table 1 summarizes their derived line parameters. Although all spectra were obtained with channel separation of 0.008 km s^{-1} they have been smoothed to lower resolutions of 0.015 to 0.025 km s^{-1} to improve their signal to noise ratio. In the top panel are shown the highest resolution spectra ($\sim$ 0.015 km s^{-1}) in 1,149S, and in the TMC-1(core-D) at 72 arcsec to the south-east of the nominal center. All these spectra are fully resolved even though their total width is very narrow (< 0.8 km s^{-1}). Except for L1498 all profiles show evidence for the presence of multiple components. L1498 is the smallest core in this sample (size 3.6 arcmin) and has the narrowest spectrum (Fig. 1a). Its width could be as narrow as 0.135 km s^{-1}, as seen in the individual spectra before averaging. The profile of L1498 appears to be that of a single velocity component (although there could be two others). 011 the other hand 1,1544, 1,1521 B, and TMC-1 exhibit several distinct velocity components. Furthermore, parts of their profiles suggest the presence of very narrow gaussian width components. For example, as shown in Fig. 1b the sharp edges of TMC-1 profile can be well fitted with a gaussian with half-width of 0.15 km s-]. Therefore, we conclude that the narrowest features in these spectra have a characteristic line width of NO.] 5 km s^{-1}, and interpret it as the intrinsic line-width of a typical coherent strut.turc (clump) within the core. While it is possible to fit the narrowest features in these profiles with line widths [1OWJI to **0.10** km s^{-1}, widths > 0.15 km s^{-1} produce poor fits with excess residuals at the edges of the profiles. Therefore for the discussions presented here we assume the intrinsic CCS linewidth for the clumps to be 0,15 km s^{-1}.

These dark cloud cores arc believed to be very cold, with gas kinetic temperatures typically $\sim$10 K (B enson and Myers, 1989). Pure thermal broadening for CCS at this temperature is about 0.09 km s^{-1}. Therefore our results S]1OW that the non-thermal broadening is $\leq$ 0.1 km s-]. The non-thermal broadening may be due to turbulence, rotation, infall and outflow; thus turbulence, if present at all, is $\leq$ 0.1 km s^{-1}.

3.2 Separation of clumps

3.2.1 Decomposition of single line profiles

The high resolution and high signal to noise ratio in these spectra allow us to decompose line profiles into individual velocity components which are seen in superposition along the line of sight within the antenna beam area. In the lower panel of Fig. 1 (c & d) the relative intensities and velocities of the decomposed components (clumps) are indicated by gaussian profiles. The decomposition has been made by deconvolving the line profiles with a gaussian of width (FWHM) 0.15 km s^{-1} corresponding to the assumed maximum intrinsic line profile of a single component. We used the iterative CLEAN algorithm

(Högbom, 1 974) for deconvolution. Using a smaller width of 0.10 km s^{-1} for the deconvolving gaussian produced similar results in terms of the number of components and their velocities, but changed the relative intensities. Larger intrinsic widths produced fewer components, but resulted in poor fits and significantly large residuals. The fits shown in Fig. 1 demonstrate clearly the clumpiness and velocity structure in these cores. The parameters derived from CCS spectral line profiles are given in Table 1. We assume that in a single spectrum we are able to detect all the components within the beam (corresponding to about 1 arcmin diameter). The total number of clumps in each core given in Table 1 has been estimated using this assumption. The large number of clumps within the cores (> 1 00) indicate a high degree of fragmentation.

3.2.2 Decomposition of Position-Velocity Maps

The clumps appear to be spatially unresolved (see below) and therefore, the T_A of any velocity component in the profiles in Fig. 1 will be diminished if it is located away from the the center of the beam. To gain more insight into the clumpiness and velocity structure than what is inferred from the single spectral line profiles shown in Fig 1, we have also made CCS position-velocity maps with Nyquist sampling at every 24 arcsec.

As an example, Fig. 2 shows a position-velocity map in TMC-1C along the east-west direction through the center of the core. The spectra at position offsets of 24 arcsec to the east and west, along with the deconvolved gaussians, are also shown (Fig. 2c & d), so that the velocity components seen in the single profiles can be traced in the P-V map. Fig. 2b shows the distribution of the clumps (velocity components) obtained by deconvolving the]mitiol)-velocity map (Fig. la) using a 0.15 km s^{-1} wide gaussian for the intrinsic line profile of a single clump, as described in the previous section. However, in this case we have also used the fact that the clumps appear in adjacent spectra, with their intensity following the antenna beam pattern. This provides a more stringent constraint 011 the deconvolution than for the single spectra. Thus the CLEANed and restored position-velocity map (Fig. 2b) represents the clump distribution and the velocity structure. We have derived similar maps of the clumps in TMC-1 (core-D) and B335 (c.f. Velusamy et al. 1 993) and the results will be presented elsewhere.

As seen from Fig. 2 the decomposition of the velocity components in the single line profiles is quite consistent with that derived from the P-V maps. From Fig. 2b we determine that there are about 16 clumps with $T_A \geq 0.5$ K (within 1 x 5 arcmin^2) and we estimate a total of about 170 clumps within 12.6 x 4.1 arcmin^2 size of this core, consistent with the estimate obtained by scaling the number of components in a single spectrum. Therefore, the total number of clumps in the cores given in 'J'able 1 estimated from scaling a single spectrum should be reliable within a factor of 2. These maps with position off-set along only one direction, do not have the true T_A for all the clumps. Ideally we need 3- dimensional spatial-velocity cubes to investigate fully the true brightness of all the clumps. Nevertheless, our maps clearly bring out the clumpiness present in these cores and their velocity distribution.

3.3 Size and mass of the clumps

In view of the crowding of the clumps it is difficult to estimate their size reliably. We place an upper limit of 30 arcsec as the clumps appear to be unresolved (in the deconvolved

l'-V maps an unresolved clump would appear as a gaussian with FWHM of 45 arcsec along the position axis). In core-D of TMC-1 the highest brightness of the deconvolved clumps is about 1.5 1{. It is likely that the clumps have optical depth $\tau \geq 1$ (inferred from the limit given by Suzuki et al. (1 992) using lower spatial and spectral resolution for this transition) and that their T_A approaches the excitation temperature in the range of 4.0 to 6.3 K (derived by Hirahara et a]. 1992). In that case the low brightness observed (less by a factor of 4 than T_{ex}) is due to the beam dilution and places a stringent upper limit of about 22 arcsec for the angular size of the clumps.

In Table 1 we give estimates of upper limits for the mass of the clumps obtained by dividing the masses of the cores by the total number of clumps determined from the line profiles. For the total mass of the cores we have used the values from Benson and Myers (1989) as well as the virial masses estimated from the line widths given in column 4 in Table 1. The mass of core-l) in TMC-1 was estimated using the mean density $n(H_2) \sim 4 \times 1\ 0^4\ cm^{-3}$ given by Hirahara et al (1 992). Since we have assumed that all the mass of the core is in clumps the values in Table 1 for the clump mass are upper limits.

If we assume an angular size of 22 arcsec (0.015 pc at the distance of TMC-1) for the clumps then using the mean density in the TMC-1 core we get a lower limit estimate of **0.003** $M_\odot$ for the clumps. However this estimate is uncertain by an order of magnitude if the clump size or the density or both should be different. Obviously, the density in the clumps will be higher than the mean density ($\sim 4 \times 10^4$ cm^{-3}). In the position-velocity maps of the clumps (Fig. 2b), we find the ratio of the clump to inter-clump brightness varies from 2 to 5 (the inter clump brightness is about 0.3 1{). The true brightness of the clumps may be much higher ($\geq$ a factor 4) when corrected for beam dilution. Assuming constant fractional abundance of CCS in the core this brightness variation may be interpreted as density contrast between the clump and inter clump-region. Therefore, the density in the clumps is likely to be higher by a factor of 10 than the mean density in the core. However, as the angular size of the clumps are likely to be smaller, these mass estimates will not increase by more than a factor of a few. If we assume the turbulence to be $\sim$ **0.1** kms^{-1} within a clump (after allowing for thermal broadening and systematic velocity motions, rotation, infall, outflow, etc.) we estimate the virial mass in a single clump to be $< 0.04\ M_\odot$, for clump size < 30 arcsec. From all the above consideration, and the estimates in Table 1, we conclude that the limits for the mass of the clumps are in the range between 0.003 and 0.04 $M_\odot$; hence, the mass of the clump is most likely to be of the order of 0.01 $M_\odot$.

4 Discussion

The critical mass and radius for collapse of a 20 K cloud core is about 30 $M_\odot$ and 0.3 pc. However once it starts to collapse , the critical mass for collapse decreases as the collapse proceeds, and breaks up into smaller fragments of smaller mass, which could themselves collapse independently. These fragments in turn become liable for further fragmentation. However, the process of hierarchical fragmentation will ultimately be halted as part of the gravitational potential energy is converted into heat. The lowest mass possible to form by successive fragmentation is about 0.01 $M_\odot$ (Spitzer 1988; Rees 1976; Low and Lynden-Bell 1976).

It is intriguing that the masses of the lowest sub-units (fragments) thus formed by

successive fragmentation, are comparable to the clumps detected in the CCS spectra. However, the theoretical limiting mass for fragmentation has been derived on the assumption of high density $\sim 10^{10}$ cm^{-3}, and cooling by emission from optically thick dust, but detection of CCS emission from the clumps indicate a much lower density (104 - 106 cm^{-3}). Nevertheless, it seems possible that the successive fragmentation may also result in long lived quasi-stable low mass fragments with density of 105 to 10^6 cm^{-3}. At densities < 104 cm^{-3} the molecular line emission from CO, CS, O_2, etc., is very efficient for cooling, but at densities $\geq 10^4$ - 10^5 cm^{-3} become less efficient (Goldsmith and Langer 1978). At low gas temperature ($\leq$ 10-20 K), it is possible to balance (or at least slow) the further collapse of the fragment. A comparison of the thermal time scales, with the free fall times, and sound speed in this density regime indicate that these fragments are likely to be stable, with lifetime of 10^5 yr, as they are confined externally by the inter-clump gas (Langer et al. 1993). As seen from the maps of TMC-1C (Fig. 2b) and core-D in TMC-1, a large fraction (about 50 percent) of the mass in these cores are in the clumps and hence are completely fragmented to the smallest possible limit. If star formation is to take place here these fragments must coalesce to gather sufficient mass for protostellar collapse. If the molecular clumps are indeed quasi-stable, as described above, there may be enough time for coalescence to lead to a protostellar object.

We would like to thank members of the HRMS and DSN staff for their help with the operation the 70 m-antenna and WBSA. We also appreciate the support and encouragement of Drs. S. Gulkis and M. Klein of JPL. This research was conducted while T.V. held a National Research Council Senior Research Associateship. This research was performed at the Jet Propulsion laboratory, California Institute of Technology, under contract with National Aeronautics and Space Administration.

References

[]] Bensen, P.J, & Myers, P.C. 1989, ApJ.Suppl., **71** , 89.

[2] Goldsmith,P.F., & Langer, W.D. 1978, ApJ 222, 881.

[3] Hirahara,Y., Suzuki,]]., Yamamoto,S., Kawaguchi,K., Kaifu,N., Ohishi,M., Takano,S., Ishikawa,S., & Masuda,A. 1992, ApJ 394 , 539.

[4] Högbom,J.1974, Astr. AstI"o]dIy.Su]@.,15,417.

[5] Langer, W.D., Velusamy,T., & Kuiper,T.B.H. 1993, in preparation.

[6] Low,C., & Lynden-Bell,D. 1976, M.N.R.A.S. **176**, 367.

[7] Quirk,M.P., Wilk,M.F., Garyantes,M.F., & Grimm,M.J. 1988, IEEE '1'rails, on Acoustics, Speech and Signal Processing, 36, 1854.

[8] Rees,M.J. 1976, M.N.R.A.S. 176,483.

[9] Spitzer,L.Jr. 1988 "Physical Processes in the Interstellar Medium" John Wiley & sons, New York.

[10] Suzuki,]]., Yamamoto,S., Ohishi,M., Kaifu,N., Ishikawa ,S., Hirahara,Y., Takano,S., & Masuda,A. 1992, ApJ 392, 551.

[11] Velusamy,T., Kuiper,T.B.H., Langer,W.D., Levin,S., & Olsen,E. 1993, BAAS, 25, 859.

5 Figure Captions

Figure 1. Ultra-high resolution CCS(J_N = 2_1 - 1.) spectra of dark cloud cores at 22 GHz. The spectra have been smoothed to a velocity resolution of 0.015 and 0.025 km s^{-1} as indicated. The observed spectral line profiles are shown by thick lines. Gaussian fits to the profiles or to parts of them are indicated by thin lines. The intensities are in units T_A in K. The velocity range is 1.7 km s^{-1} centered at the nominal V_{lsr} of the cores. The RA(1 950) and Dec(1950) of the source position are indicated. The gaussians fitted to (a) the narrowest spectral line in L1498 and (b) the sharp edges of the profile i*, TMC-1, have FWHM of 0,15 km s^{-1}. The gaussian curves shown under spectral line profiles (c) 1,152111, and (cl) 1.1544, represent the deconvolved velocity components (clumps) each with intrinsic line-width of 0.15 km s^{-1}.

Figure 2. Velocity structure of TMC-1 C. (a) Position-Velocity map. The position offsets are along the east-west direction (east at top), and centered at R. A.= 04''38'''30^s.0 and, Dec.= 25 °54'58". The velocity and spatial resolutions are 0.025 km S-l and 45 arcsec respectively. The first contour and contour interval are 0.15 K in T_A. (b) The velocity structure of clumps derived by deconvolving the P-V maps using CLEAN and assuming an intrinsic line-width of 0.15 km s^{-1} for each clump. For comparison to the P-V maps we show the line profiles and their velocity components at position offsets of 24 arcsec to the (c) east and (d) west.

'J'able 1

Summary of spectral line profiles

Cloud core	V_{lsr} (kms^{-1})	T_A (K)	*Line width*[b] (kms^{-1})	*Core radius* (*arcmin*)	*No. of clumps. in core*[c]	*Core mass* $M_\odot$	*Clump mass*[d] $M_\odot$	*Clump mass*[e] $M_\odot$
TMC --- la	5.83	3.25	0.72(0.50)	2.8	150	5.3	0.07	0.04
*L*1498[f]	7.84	1.69	0.35(0.16)	1.5	-	0.82	--	-
1,1.521 *B*[g]	6.45	1.83	0.66(0.42)		-	-	-	
TMC--1*C*	5.36	2.45	0.58(0.27)	3.6	150	10.0	0.07	0.01
*L*1544	7.18	1.38	0.64(0.46)	2.5	I 20	1.2	0.01	0.03
*L*1529	6.13	1.06	0.60(0.31)	3.6	250	16.0	0.06	0.01

[a] position of core-D in CCS map of Hirahara et al (1 992).

[b] width at base; value assumed for virial mass is given within parenthesis.

[c] total number estimated using core radius and components in a single profile.

[d] estimated assuming core mass obtained from mean densities.

[e] estimated assuming virial mass of the core.

[f] number of clumps not given; profile appears to have one component though it could be due to superposition of multiple components with low velocity dispersion.

[g] total number of dumps not given; profile shows at least 4 components; core parameters not available.

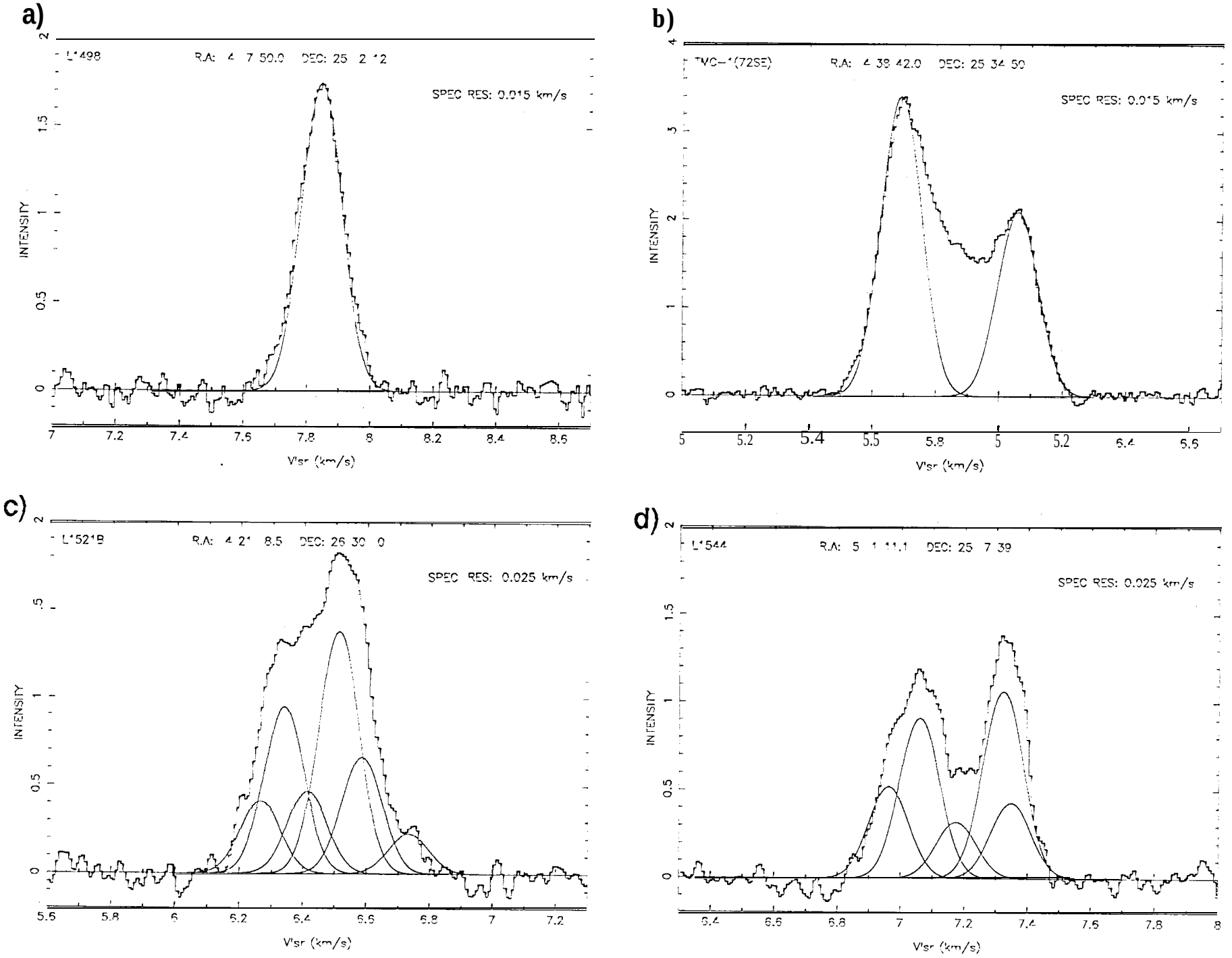
a)
L*498
R.A: 4 7 50.0 DEC: 25 2 12
SPEC RES: 0.015 km/s
INTENSITY
V'sr (km/s)
b)
TMC-1(72SE)
R.A: 4 38 42.0 DEC: 25 34 50
SPEC RES: 0.015 km/s
INTENSITY
V'sr (km/s)
c)
L*521B
R.A: 4 21 8.5 DEC: 26 30 0
SPEC RES: 0.025 km/s
INTENSITY
V'sr (km/s)
d)
L*544
R.A: 5 1 11.1 DEC: 25 7 39
SPEC RES: 0.025 km/s
INTENSITY
V'sr (km/s)

Fig. 1

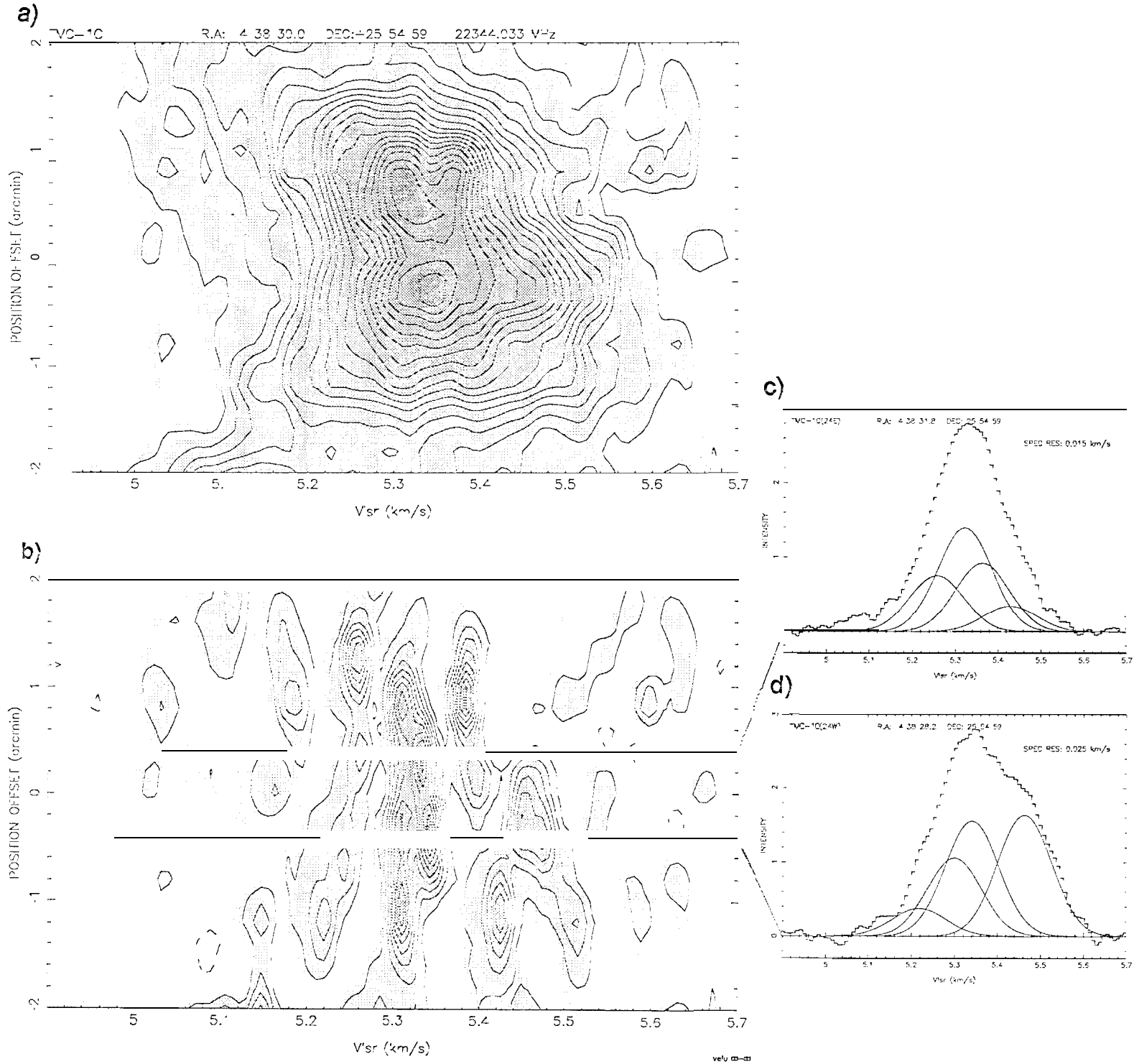
a)
VC−1C
R.A: 4 38 30.0 DEC:+25 54 59 22344.033 MHz
POSITION OFFSET (arcmin)
Vsr (km/s)
b)
POSITION OFFSET (arcmin)
Vsr (km/s)
c)
SPEC RES: 0.015 km/s
INTENSITY
Vsr (km/s)
d)
SPEC RES: 0.025 km/s
INTENSITY
Vsr (km/s)

Fig. 2